Electronic Supplementary Material (ESI) for New Journal of Chemistry.

Mechanochemical method: a powerful tool to obtain ω-poly (ethylene glycol) functionalized structures and curcumin analogues

Aniele de Moura[a], Caroline Gaglieri[a], Luiz Octávio Terciotti[a], Daniel Rinaldo[b] and Flávio Junior Caires [a,b]*

[a] *School of Sciences, Chemistry Department, UNESP, São Paulo State University, Bauru, São Paulo, Brazil*

[b] *Institute of Chemistry, UNESP-São Paulo State University, Araraquara, 14800-900, SP, Brazil*

Summary

Supplementary Figures....3

Figure S1- ^{1}H NMR spectrum of PEG_SA milled in different times (15, 30, 45, and 60 minutes) in comparison with PEG and SA spectra. 3

Figure S2- MIR spectra obtained for PEG and modified PEG with anhydrides. 4

Figure S3- ^{1}H-NMR spectra obtained for modified PEG with anhydrides *a)* PEG_AS, *b)* PEG_MA, and *c)* PEG_TCA.....5

Figure S4- MIR spectra of Curcumin, 4-formylbenzoic acid, and uracil in comparison with mixture d (DCURAC-DMCURAC-DBCURAC). 6

Figure S5- DCURAC-DMCURAC-DBCURAC ^{1}H NMR full spectrum. 7

Figure S6- DCURAC-DMCURAC-DBCURAC DEPTq NMR spectrum. 8

Figure S7- HPLC chromatogram of the DCURAC-DMCURAC-DBCURAC (a) and DCURGLI-DMCGLI-BDMCGLI (b) mixtures.....8

Figure S8- Mixture e (DCURAC-DMCURAC-DBCURAC) reactional mechanism suggestion (c).....9

Figure S9- MIR spectra curcumin and Glycine in comparison with mixture f (DCURGLI-DMCGLI-BDMCGLI). 9

Figure S10- XRD diffactograms of Calculated β-Glycine and γ-Glycine, in comparison with the diffractogram of the glycine used in this work.....11

Figure S11- DCURGLI-DMCGLI-BDMCGLI ^{1}H NMR full spectrum.....12

Figure S12- DCURGLI-DMCGLI-BDMCGLI DEPTq NMR spectrum.....12

Figure S13- HSQC spectrum of DCURGLI-DMCGLI-BDMCGLI. 13

Figure S14- Curcumin (CUR), DCG and Glycine (GLI) MIR spectra. 14

Figure S15- ^{1}H NMR of DCG in $CDCl_3$. 15

Figure S16- DEPTq NMR of DCG.....16

Figure S17- ^{1}H NMR spectrum of DCG milled during 5, 10, 15, 20, 25, and 30 mintues, in $CDCl_3$. 16

Figure S18- MIR spectra of DCG, PEG_AS, MONO_DCG, and DIES_DCG. 17

Figure S19- ^{1}H NMR spectra of DCG, MONO_DCG, and DIES DCG in the region between 5.50-4.00 ppm. 18

Figure S20- MONO_DCG, and DIES_DCG ^{1}H NMR full spectrum.....18

Figure S21- DEPT NMR of DCG, MONO_DCG, and DIES_DCG.....19

Figure S22- HPLC chromatogram of DCG, MONO_DCG, and DIES_DCG.....19

Supplementary Tables 20

Table S1: Reactants/ solvents used in this work.....20

Table S2: ^{13}C NMR signals of DCURAC.....20

Table S3: ^{13}C NMR signals of DCURGLI. 21

Table S4: ^{13}C NMR signals of DCG. 21

REFERENCES 22

Supplementary Figures

Figure S1- ^{1}H NMR spectrum of PEG_SA milled in different times (15, 30, 45, and 60 minutes) in comparison with PEG and SA spectra.

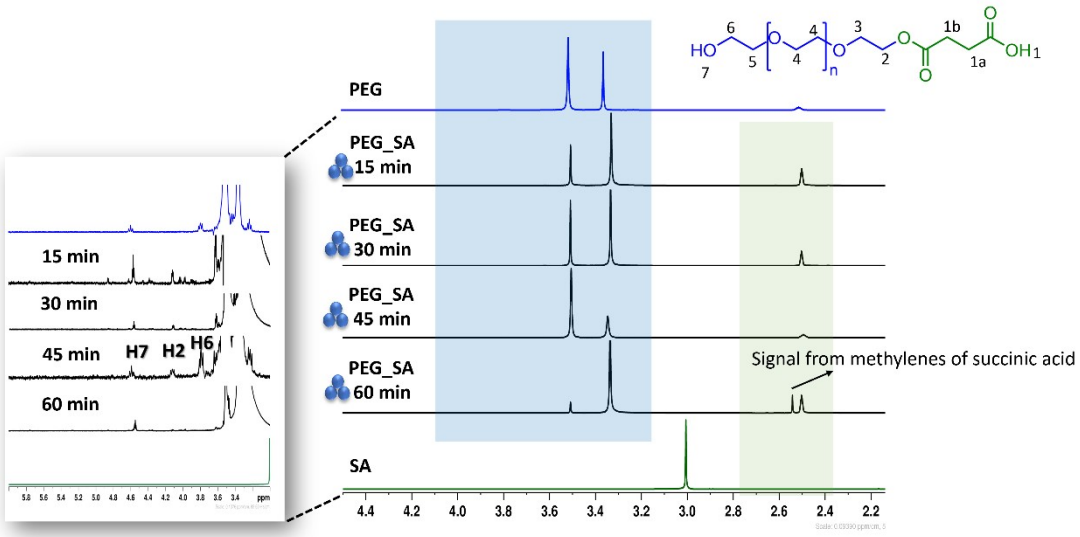

The spectra of the product PEG_SA obtained after 15, and 30 minutes of synthesis (Figure S1) do not show the triplets related to H7, H2, and H6 (showed in PEG_SA structure) at 4.59, 4.12, and 3.79 ppm, respectively, confirming that PEG_SA was not formed in these times. These signals just appeared in the spectrum of the product obtained after 45 minutes of milling. However, after 60 minutes of milling, these signals are no longer observed, suggesting that milling the sample for more than 45 minutes, can result in the mechanochemical degradation of PEG_SA.

Figure S2- MIR spectra obtained for PEG and modified PEG with anhydrides.

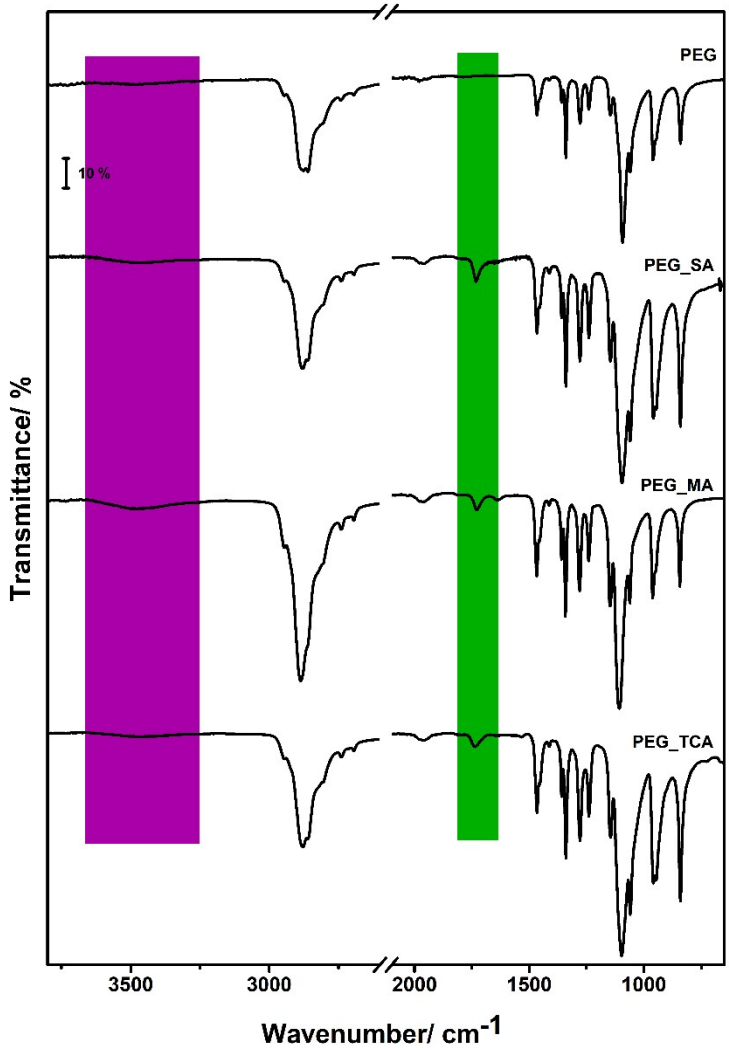

Figure S2 shows PEG_SA, PEG_MA and PEG_TCA MIR spectra in comparison with PEG spectrum. As expected, most of bands are very similar to those in PEG spectrum. The band at 1732 cm^{-1} (highlighted in green) is characteristic of carbonyl stretching (C=O) in organic acids and suggests the success of PEG esterification. In addition, it is observed a large band between 3600 and 3300 cm^{-1} (highlighted in purple) associated with the O-H stretching of the carboxylic acid present in all modified PEG structures (Figure 1).[1] These bands indicate that the esterification occurred by just one site of anhydride. Moreover, the absence of anhydrides carbonyl stretches, suggests that the products present good purity.[2]

Figure S3- ^{1}H-NMR spectra obtained for modified PEG with anhydrides *a)* PEG_AS, *b)* PEG_MA, and *c)* PEG_TCA.

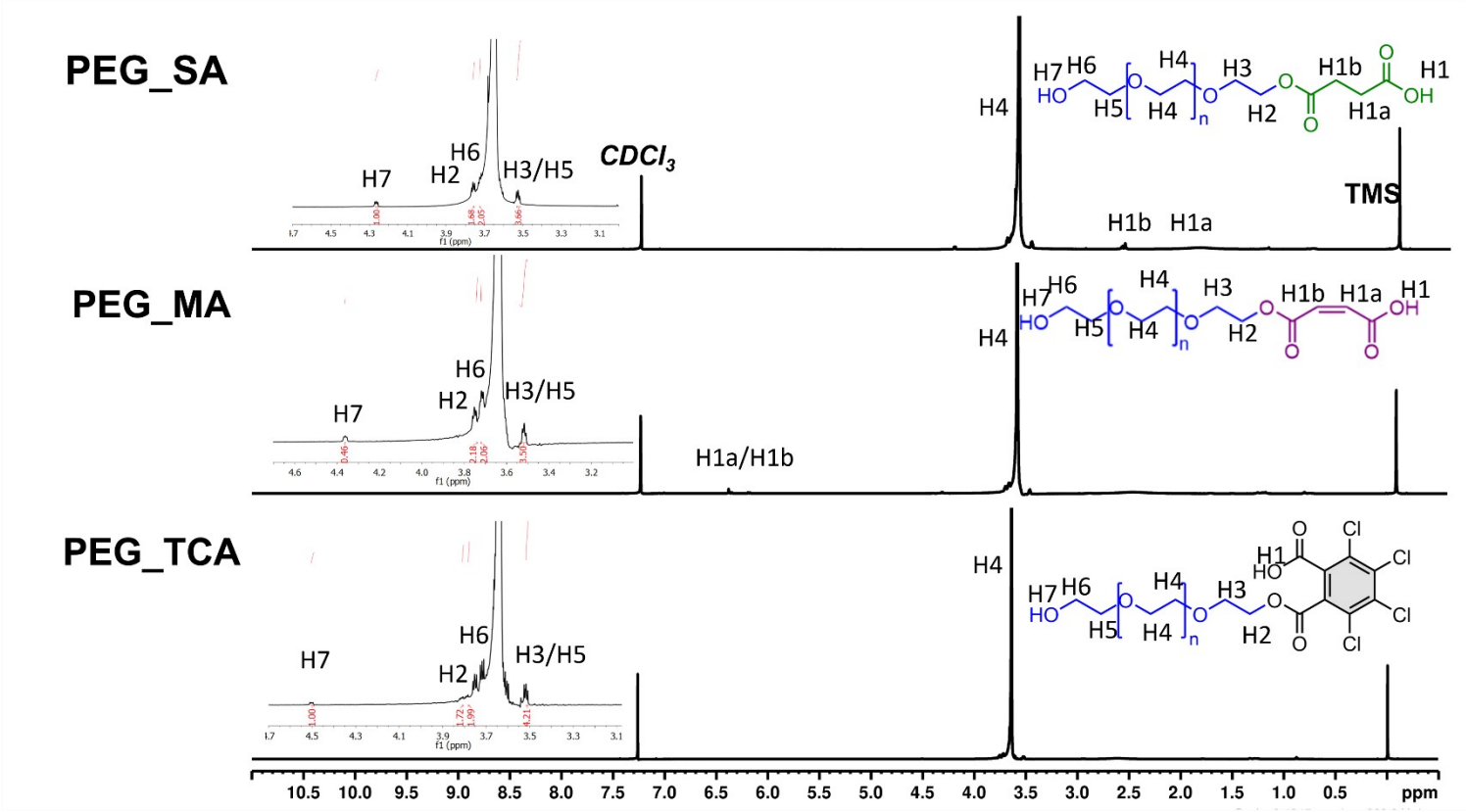

The most intense signal at 3.51 ppm observed in PEG and PEG_SA spectra is related to the -OCH_2 group (H4). The hydrogens H2/H6 and H3/H5 of PEG are observed in the triplet at 3.79 ppm and 3.23 ppm, respectively.[1,] However, these hydrogens present different chemical environments in the PEG_SA spectrum due to the nonsymmetric characteristic of the molecule. Then, the PEG_SA methylene protons H2 and H6 of PEG_SA have different chemical shift, and these signals split into two triplets at 4.12 ppm (H2) and 3.79 (H6), each one integrating to one hydrogen. Moreover, the signals of H3/H5 hydrogens are present in the triplet at 3.23 ppm. The hydroxyl hydrogen (H7) is observed in the triplet at 4.59 (∫=1). Finally, as observed in SA spectrum, the hydrogens of succinic anhydride (1a, and 1b) resulted in a unique singlet at 3.01 ppm. Therefore, in PEG_SA spectrum, these hydrogens are observed in the signal at 2.78 ppm (H1b) and 2.39 ppm (H1a).

Figure S4- MIR spectra of Curcumin, 4-formylbenzoic acid, and uracil in comparison with mixture d (DCURAC-DMCURAC-DBCURAC).

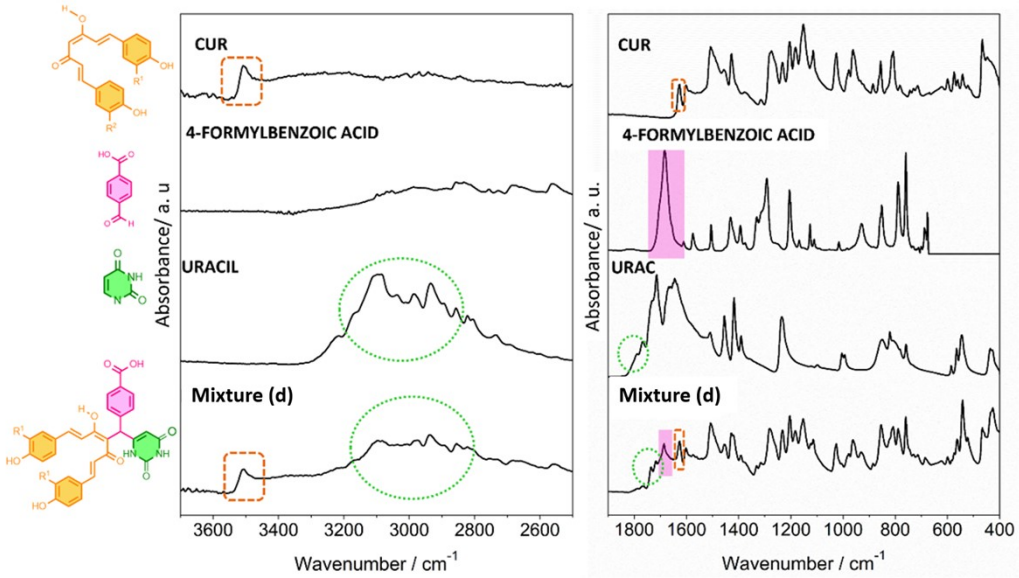

The bands at 1735 and 1716 cm^{-1} are assigned to the νC=O groups related to uracil backbone and are highlighted by the green circle.[3,4] Then, it is observed the intense band at 1685 cm^{-1}, which can be related to νCOOH stretching of 4-Formylbenzoic acid backbone, overlapped with the νC=C stretches of aromatic ring of mixture e (highlighted in pink in the spectra of 4-Formylbenzoic acid and mixture d). The band at 1626 cm^{-1} is attributed to the band νC=O from curcumin and νC=C.[5,6]

Finally, the bands at 3506 and 3096 cm^{-1} are related to the phenolic OH from curcumin backbone and νN-H from uracil backbone, respectively.[1-4]

Figure S5- DCURAC-DMCURAC-DBCURAC ^{1}H NMR full spectrum.

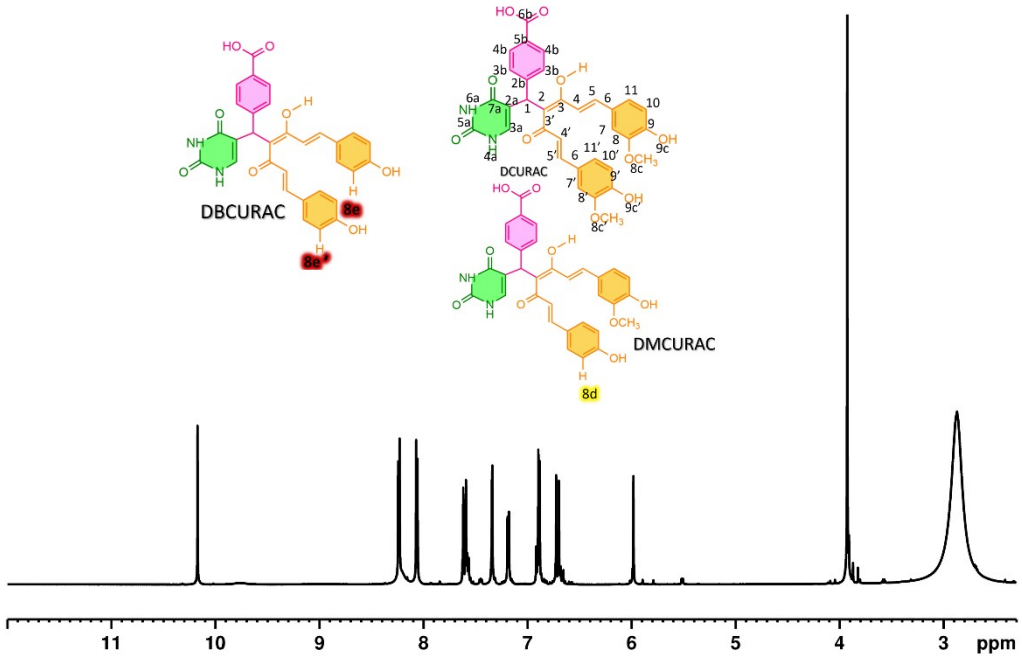

The ^{1}H NMR of DCURAC-DMCURAC-DBCURAC (Figure 4-a/S5) shows a singlet at 10.17 ppm (s,1H), which is related to the hydrogen from carboxylic acid (H7b).[7-9] In addition, the doublet signals in the region between 8.24-8.22 ppm (*d*, J = 8.3 Hz) and 8.07-8.05 (*d*, J = 8.3Hz) ppm are related to the aryl hydrogens from 4-formylbenzoic acid backbone H5b/H5b', and H4b/4b', respectively.[7-9] However, it can be observed that the doublet δ=8.24-8.22 ppm is broad, and displays an integral equal to four. This signal corresponds to the NH group (H4a/H6a) from uracil backbone, which is overlapped with the H5b/5b' hydrogens.[10,11] Additionally, the doublet δ=8.07-8.05 ppm integrating to three hydrogens is related to the hydrogen H3a, which is overlapped by the H4b/4b' hydrogens. The signals from curcumin backbone can be observed in the spectrum in the region between 7.67-5.98 ppm. The singlet at 5.98 ppm is related to hydrogen H1, and its integration equal to one confirms the compound formation with a sp^3 carbon in DCURAC structure.[7,8] The signals H8d (DMCURAC) and H8e/8e' (DBCURAC) are overlapped with other curcumin hydrogens, between 6.89-6.88 (*d*, 3H) and 6.72-6.70 (*d*, 4H), respectively.

Figure S6- DCURAC-DMCURAC-DBCURAC DEPTq NMR spectrum.

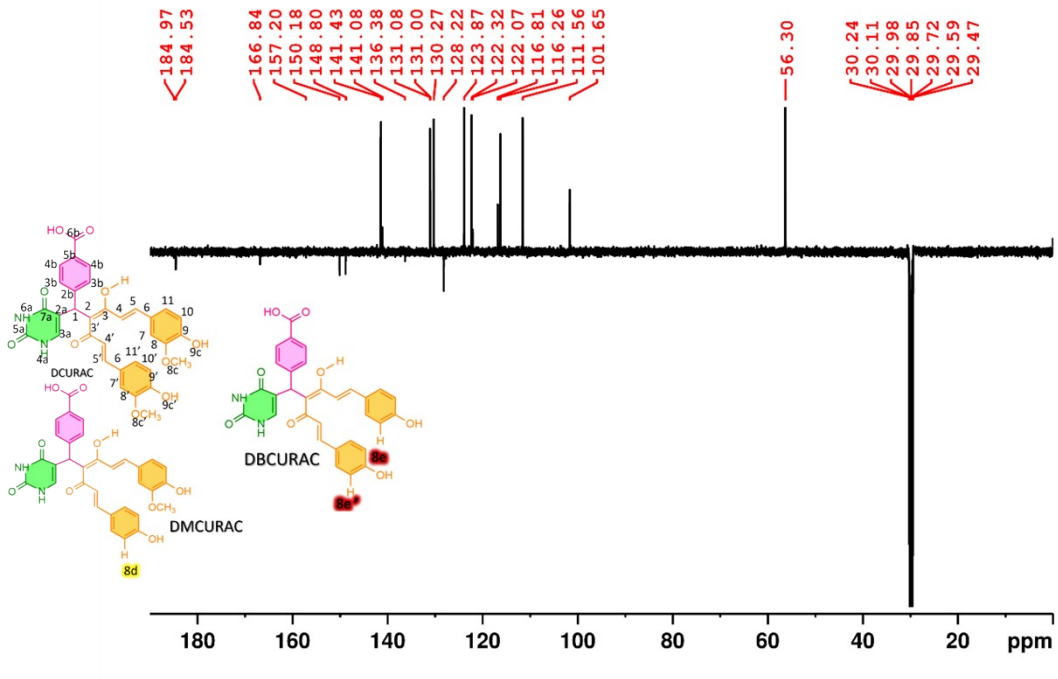

Figure S7- HPLC chromatogram of the DCURAC-DMCURAC-DBCURAC (a) and DCURGLI-DMCGLI-BDMCGLI (b) mixtures.

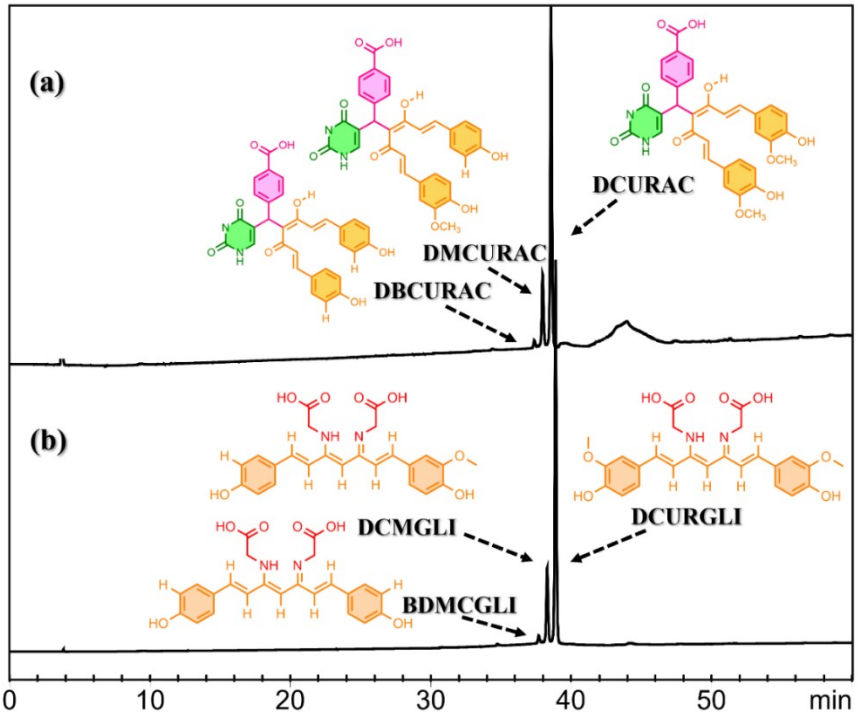

Figure S7 shows the HPLC chromatograms of DCURAC-DMCURAC-DBCURAC, and DCURGLI-DMCGLI-BDMCGLI. As aforementioned in the manuscript, both compounds display three chromatographic bands due to the reactant curcumin, that has 65% of purity, and presents in its composition DCM, and BDMC.

Figure S8- Mixture e (DCURAC-DMCURAC-DBCURAC) reactional mechanism suggestion (c).

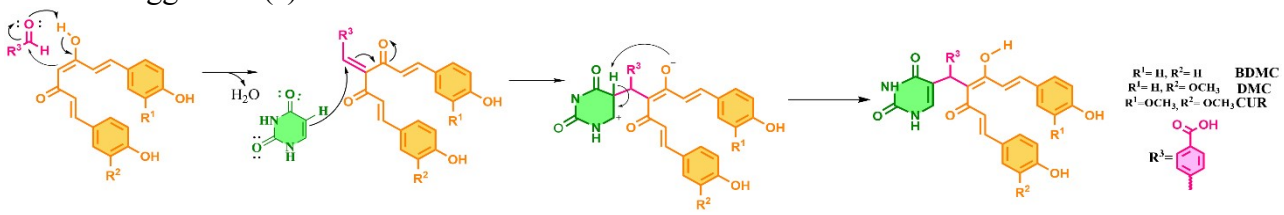

Figure S9- MIR spectra curcumin and Glycine in comparison with mixture f (DCURGLI-DMCGLI-BDMCGLI).

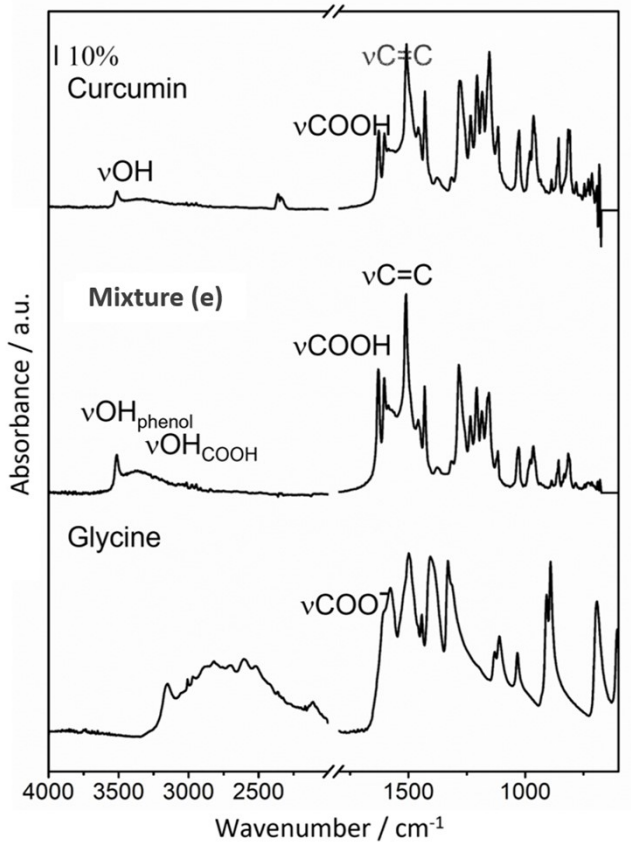

Curcumin and mixture e spectra are very similar.[5,6] The νOH phenol from curcumin backbone is observed in mixture e spectrum at 3512 cm^{-1}. Then, a broad signal between 3462-3175 cm^{-1} is observed, which may be related to the νOH from COOH. In the region between 1700-1500 cm^{-1}, it is observed the bands at 1628, 1603, 1586, and 1510 cm^{-1}, which can be assigned to the stretches νCOOH, νC=N, $\nu C{=}C_{ring}$ and $\nu C{=}C_{alkene}$. However, due to the conjugation of the molecule and the high number of functional groups that absorb in the same region, it is difficult to precisely assign each band.

From the glycine diffractograms (Figure S10) used in this work, it is suggested that it is a mixture of the polymorphs β-glycine and γ-glycine, which is related to zwitterion molecules. This result is in agreement with those previously reported by some papers.[5-7] Moreover, glycine MIR spectrum shows the bands at 1576, 1502, and 1411 cm^{-1}, which are related to νCOO-(asymmetrical), δN-H (from NH_3^+), and νCOO (symmetrical)[12-14]. Therefore, these bands confirm that the glycine used in this work presents in its composition, molecules in zwitterion form. As a result, this may make the Schiff base formation difficult, which can explain why the Schiff base (mixture e) was only formed when glycine: curcumin (4:1) proportion was higher than 4, as presented in the experimental section (it can be viewed in the manuscript).

Figure S10- XRD diffactograms of Calculated β-Glycine and γ-Glycine, in comparison with the diffractogram of the glycine used in this work.

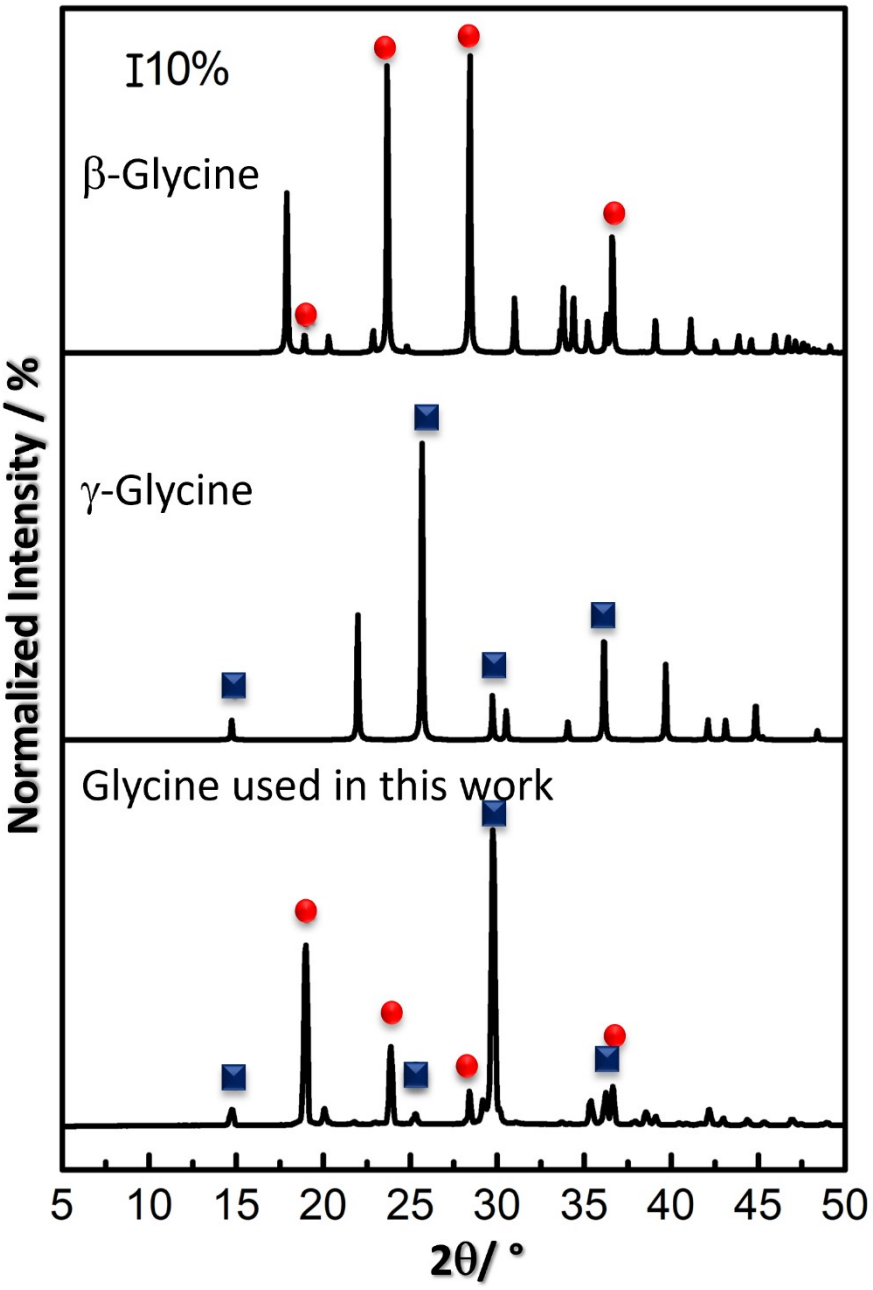

The calculated diffractogramms were obtained using the program Mercury 2020.3.0, from Cambridge Crystallographic Data Centre, by using an academic free licence,

Figure S11- DCURGLI-DMCGLI-BDMCGLI ^{1}H NMR full spectrum.

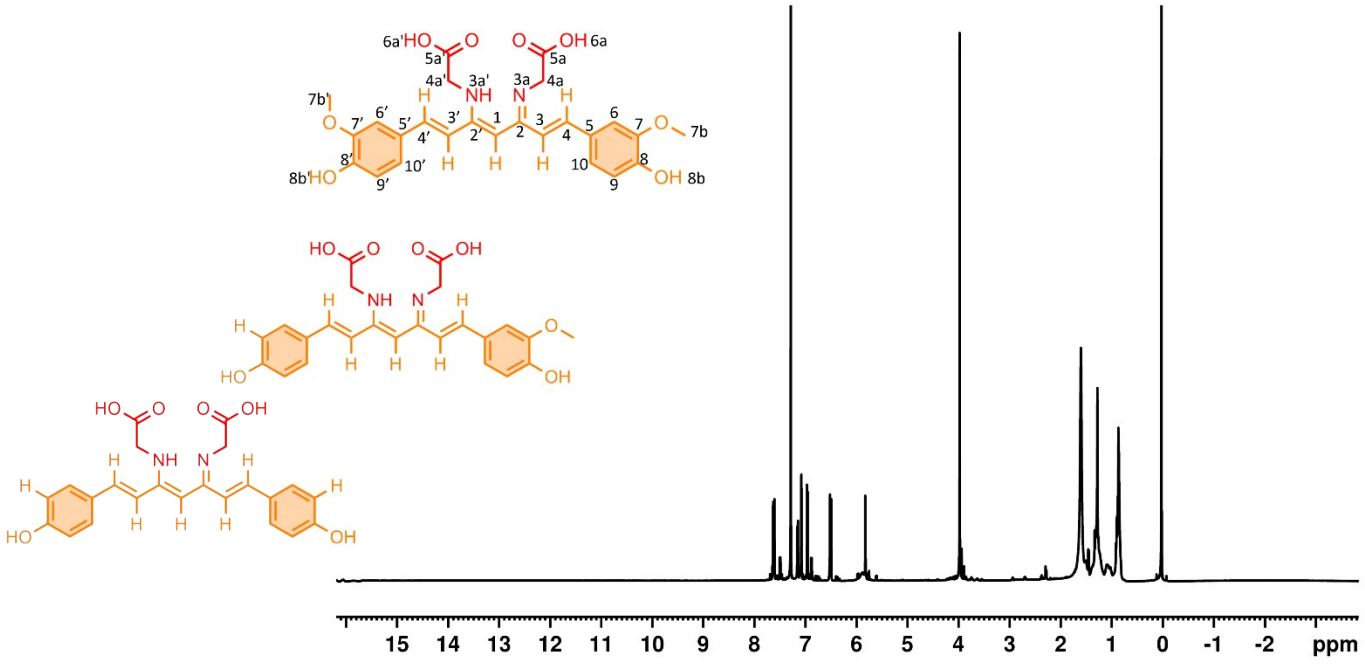

Figure S12- DCURGLI-DMCGLI-BDMCGLI DEPTq NMR spectrum.

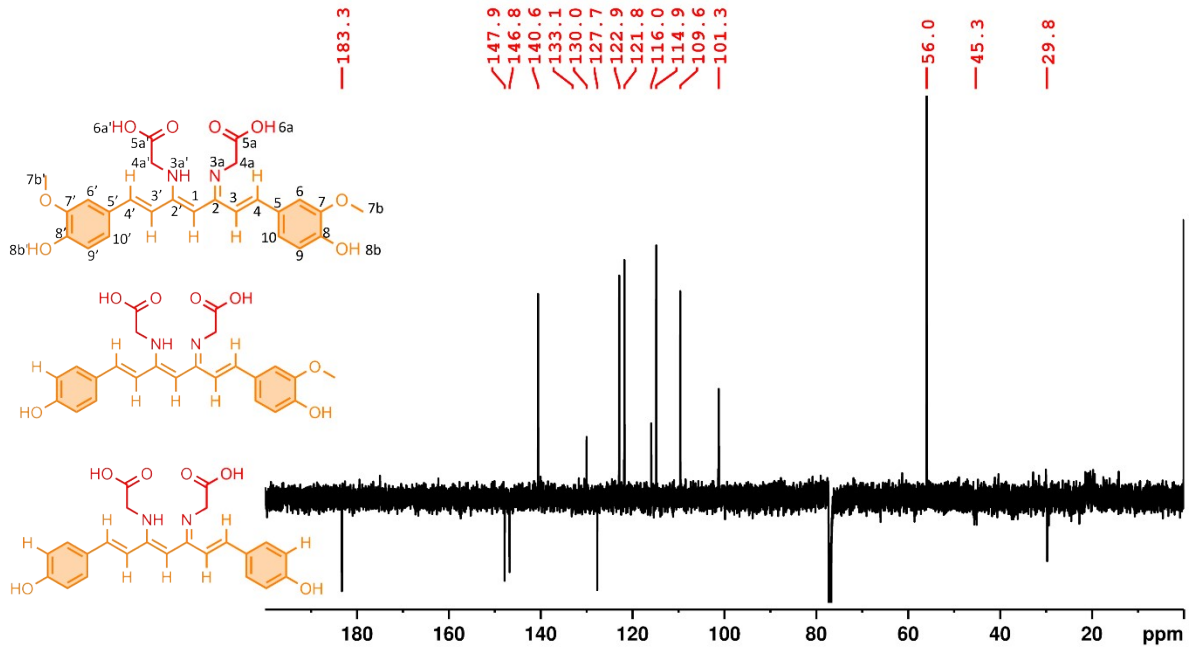

Figure S13- HSQC spectrum of DCURGLI-DMCGLI-BDMCGLI.

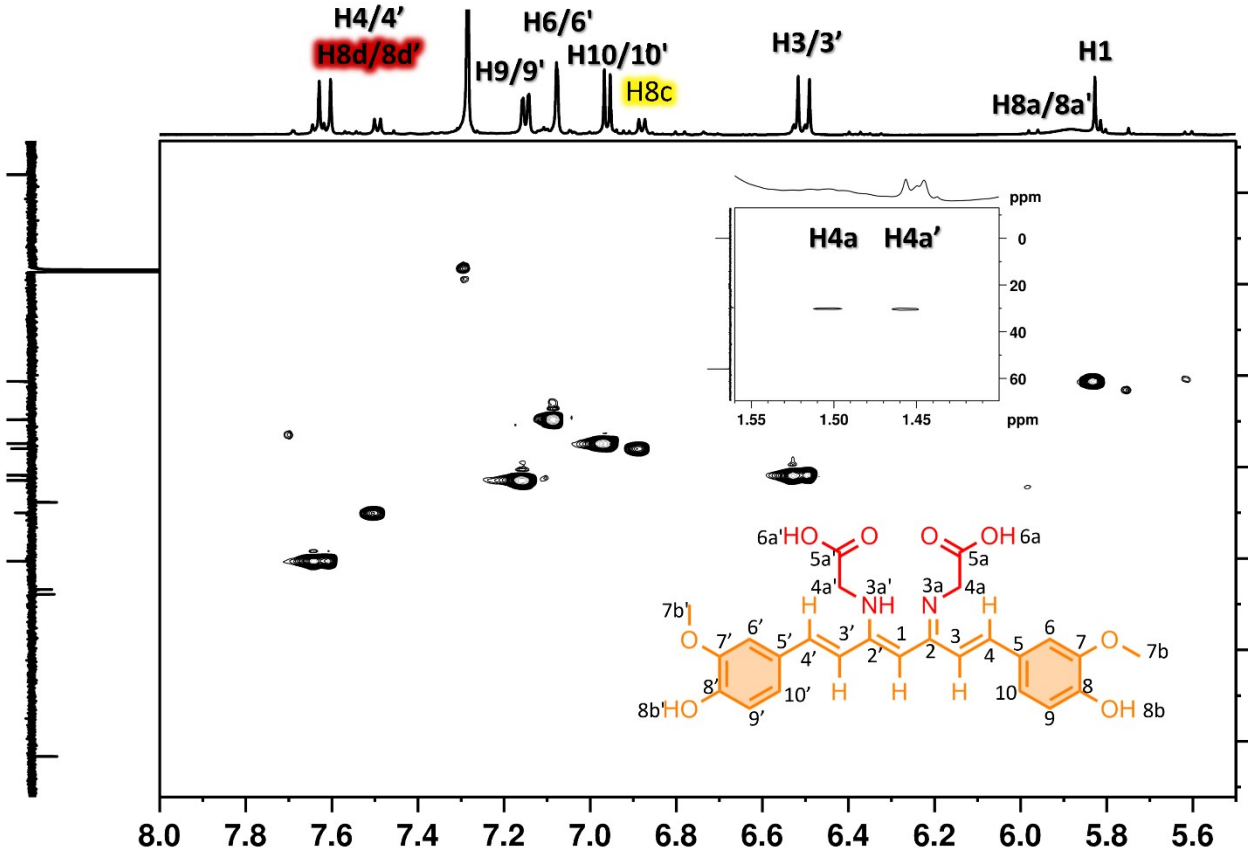

Figure S14- Curcumin (CUR), DCG and Glycine (GLI) MIR spectra.

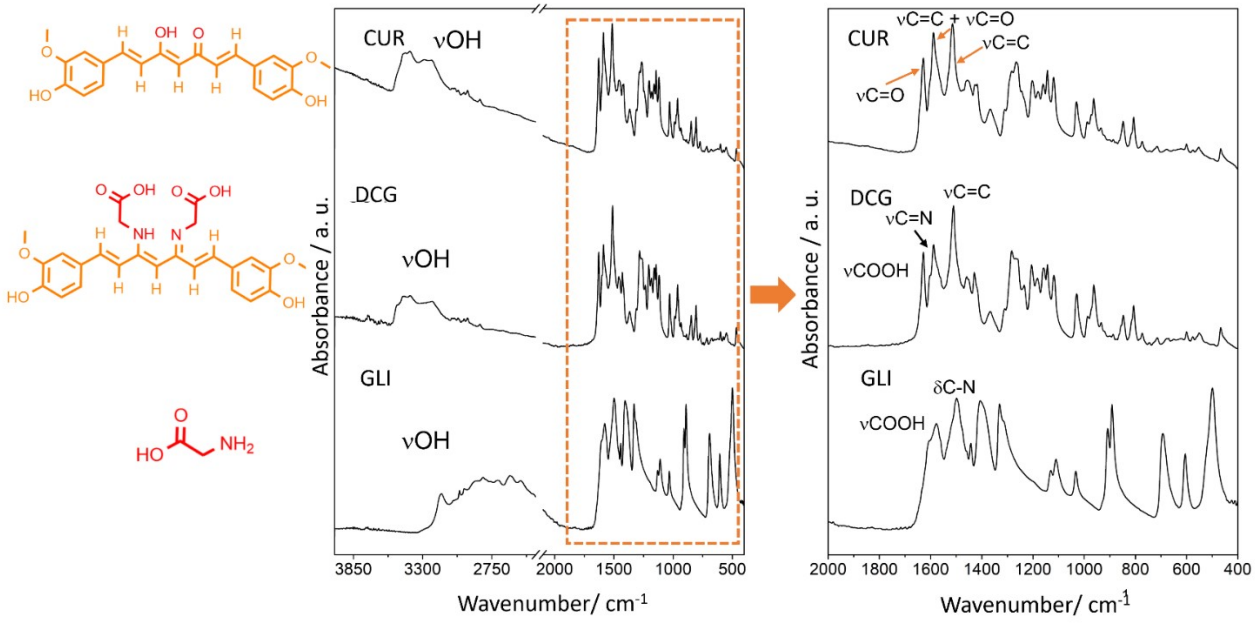

The MIR spectra of curcumin (≥92%), DCG, and uracil are displayed in Figure S15. As occurred with mixture f, DCG displays a similar spectrum when compared to curcumin. The main bands are observed at 1627, 1587, and 1509 cm^{-1}, and are related to the stretches νCOOH, νC=N, νC=C, respectively. Moreover, the band at 1587 cm^{-1} can also be assigned to $\nu C{=}C_{ring}$ stretching, overlapped with νC=N. Comparing DCURGLI and DCG MIR spectra, it can be observed a few differences, especially the band assigned to the νC=N stretch (1603 cm^{-1} for DCURGLI, and 1587 cm^{-1} for DCG).

Figure S15- ^{1}H NMR of DCG in $CDCl_3$.

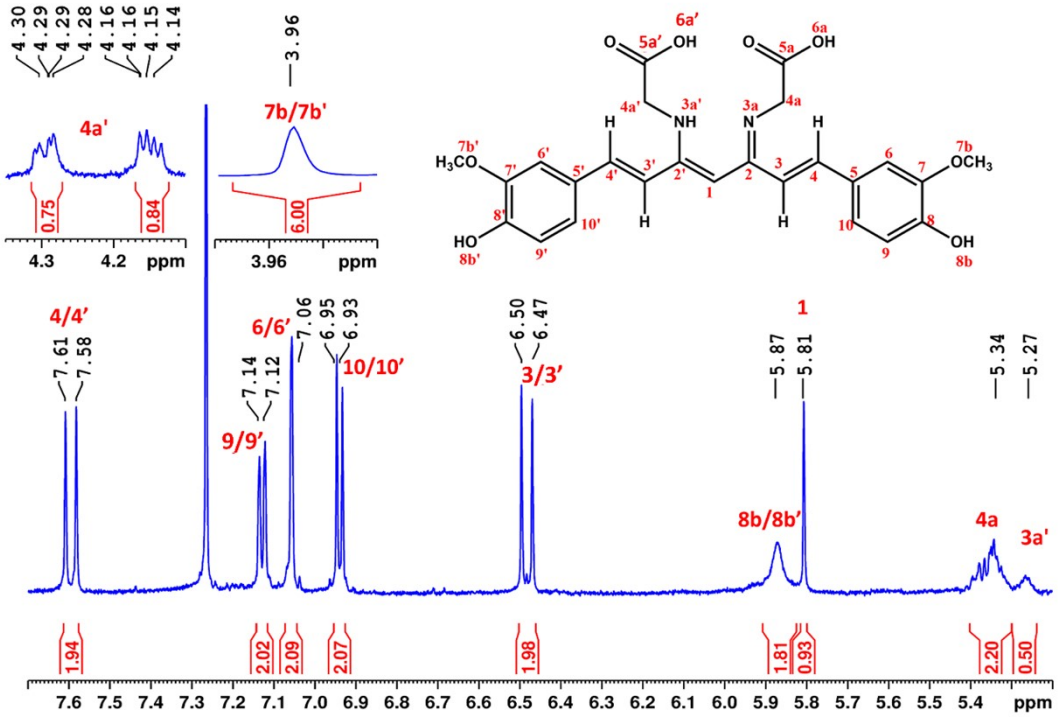

The signals related to CUR and BDMC were not observed in the spectrum in the region of aryl hydrogens (8-6 ppm), as observed in spectrum displayed in Figure 5-a for mixture f. In addition, the hydrogens of carboxylic acid were not observed. Moreover, the hydrogens of -CH_2 are observed in the signals at 5.34 ppm (*m*, 2H, 4a) and between 4.30-4.14 ppm (*m*, 2H, 4a'). The hydrogen of NH is observed as a broad singlet at 5.27 ppm.

Figure S16- DEPTq NMR of DCG.

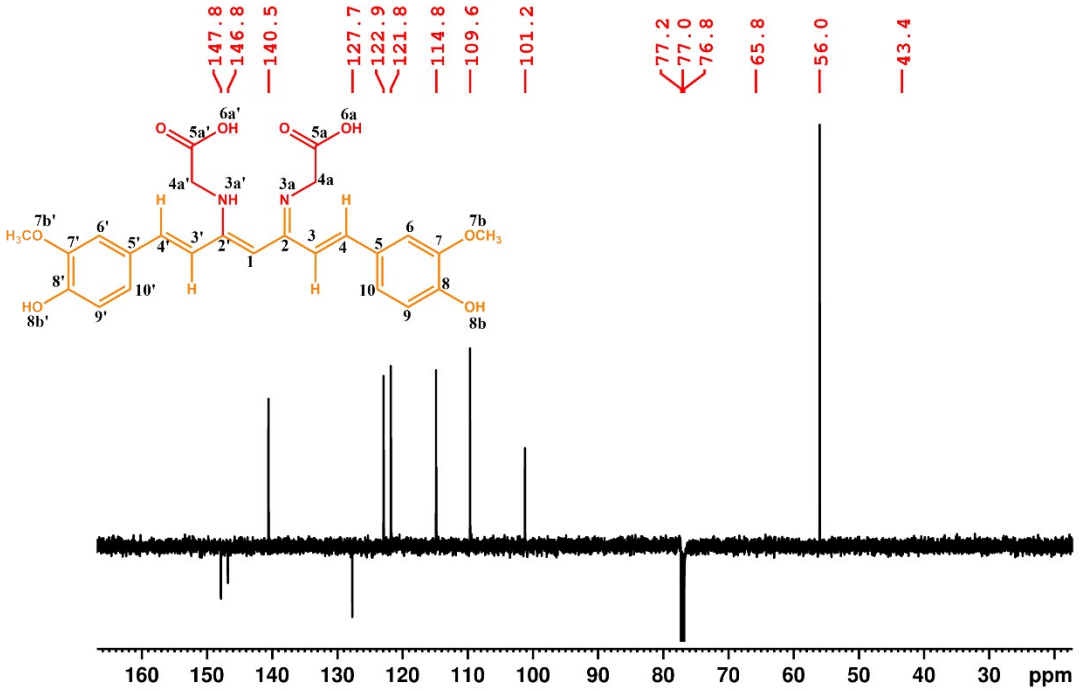

Figure S17- ^{1}H NMR spectrum of DCG milled during 5, 10, 15, 20, 25, and 30 mintues, in $CDCl_3$.

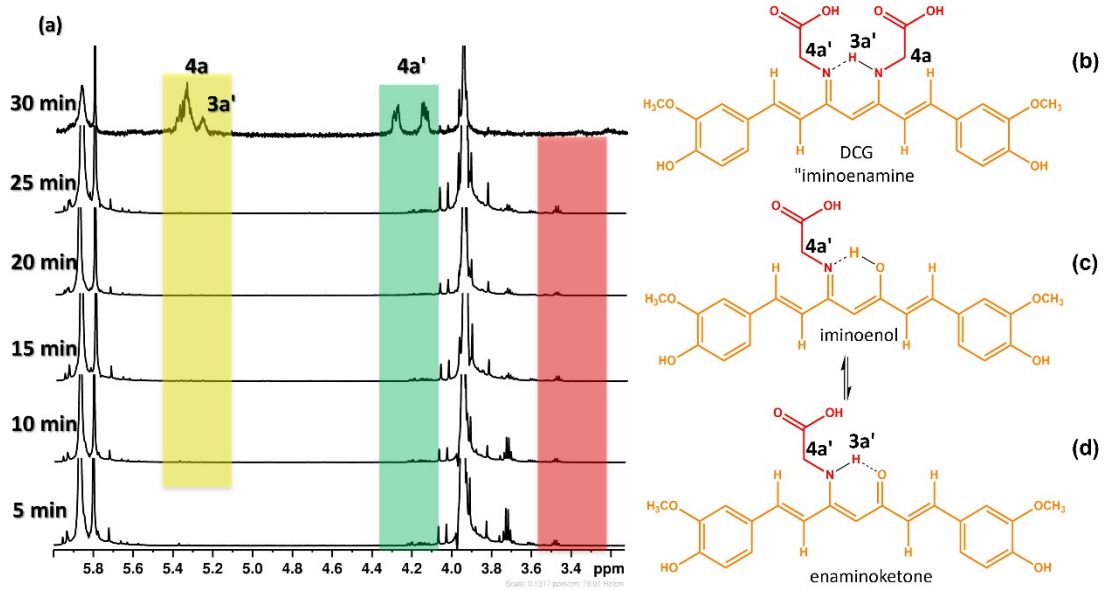

Figure S18- MIR spectra of DCG, PEG_AS, MONO_DCG, and DIES_DCG.

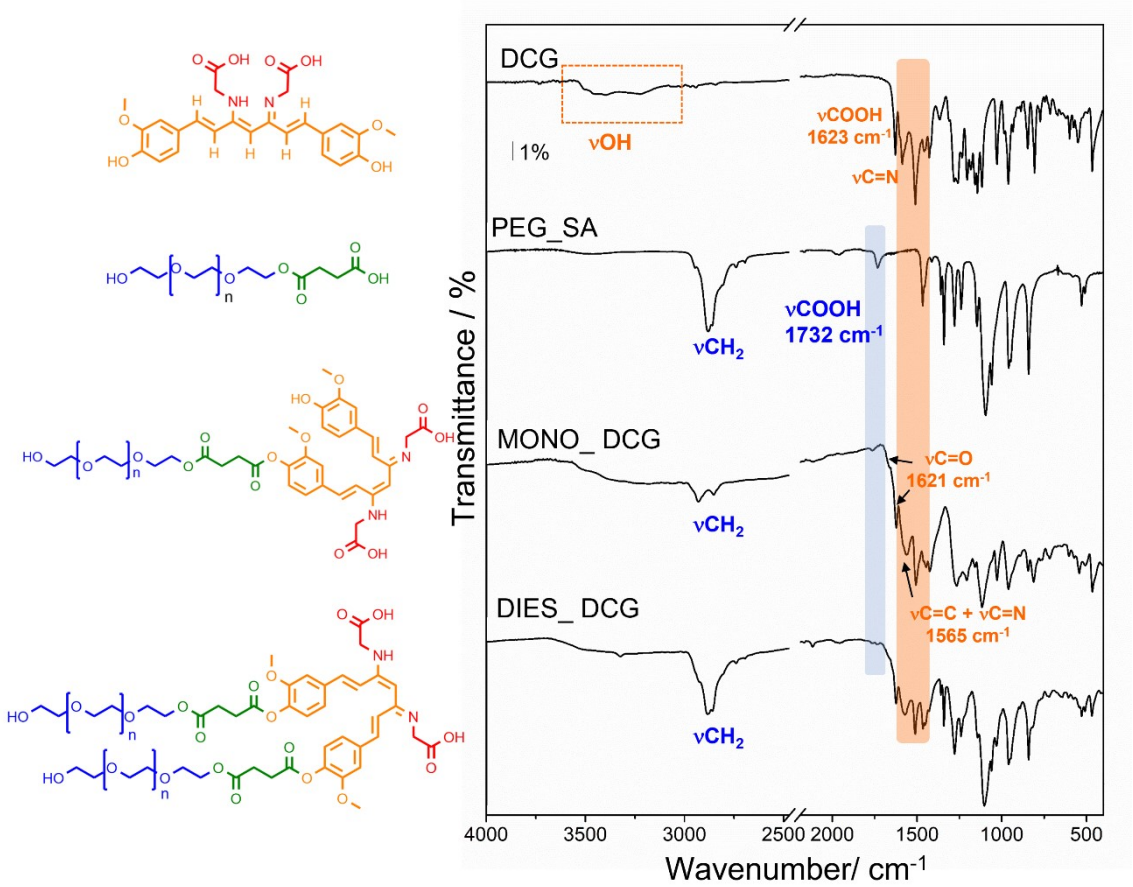

The Figure S19 displays the MIR spectra of MONO_DCG, and DIES_DCG in comparison with DCG and PEG_SA spectra. The νCH_2 band related to PEG_SA backbone at 2884 cm^{-1} is also observed in the spectra of esters MONO_DCG, and DIES_DCG. On the other hand, the band related to νCOOH present in PEG_SA spectrum (highlighted in blue) is not observed neither in MONO_DCG nor in DIES_DCG. The bands at 1667 cm^{-1} (shoulder band), and 1620 cm^{-1} observed in MONO and DIES spectra, can be assigned to the νC=O stretches related to the ester, and carboxylic acid, respectively. Moreover, the νC=N and C=C bands are probably overlapped in the large band at 1565 cm^{-1} (highlighted in orange).

Figure S19- ^{1}H NMR spectra of DCG, MONO_DCG, and DIES DCG in the region between 5.50-4.00 ppm.

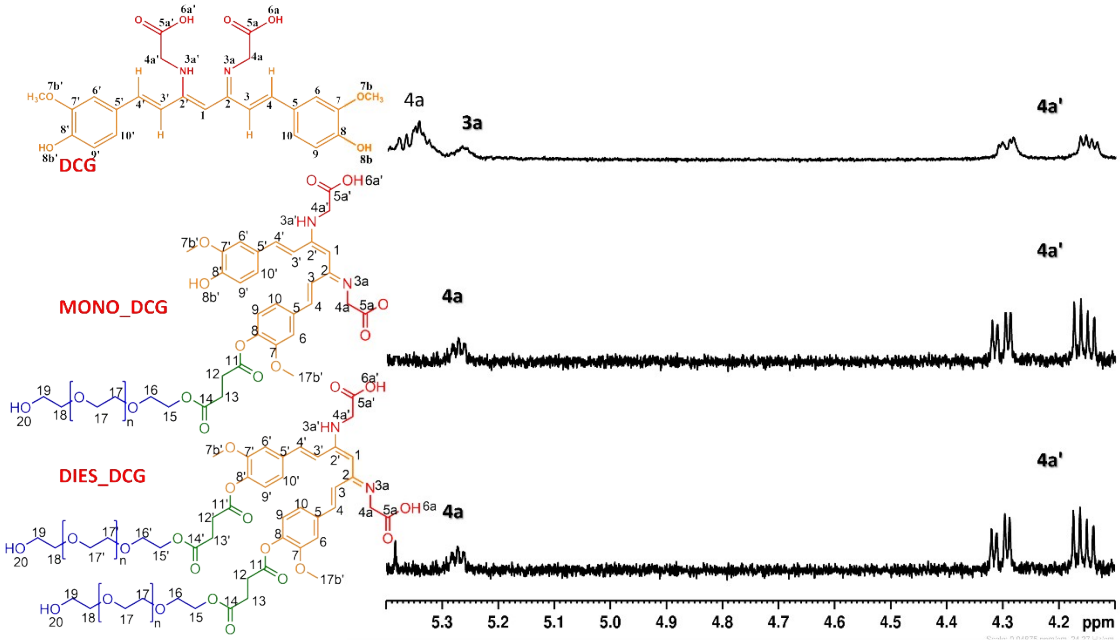

Figure S20- MONO_DCG, and DIES_DCG ^{1}H NMR full spectrum.

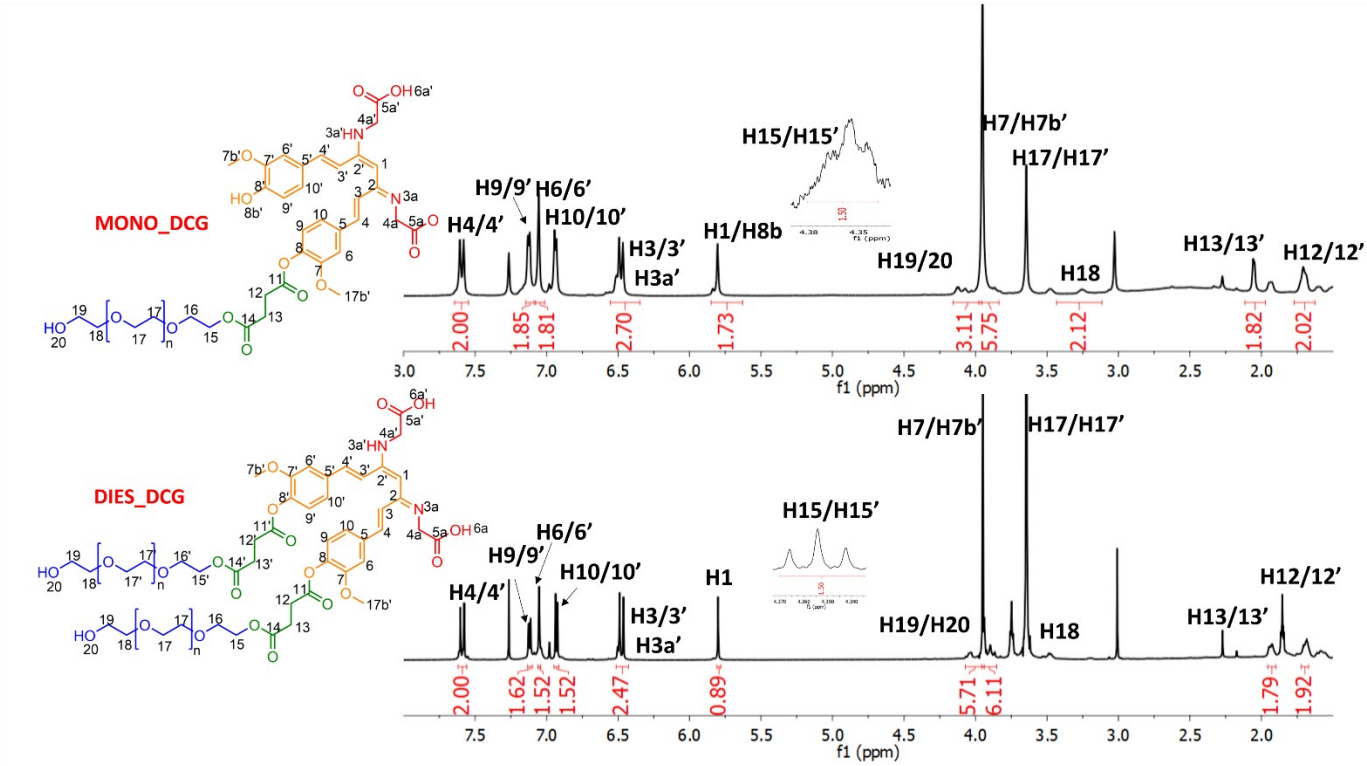

Figure S21- DEPT NMR of DCG, MONO_DCG, and DIES_DCG.

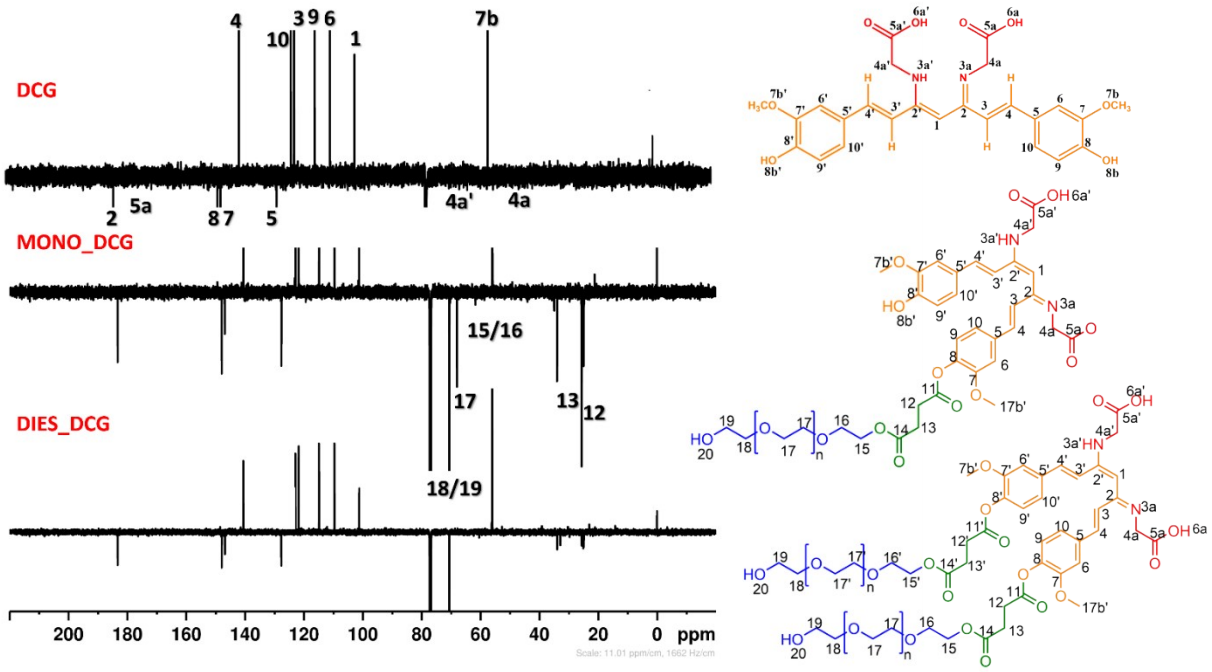

Figure S22- HPLC chromatogram of DCG, MONO_DCG, and DIES_DCG.

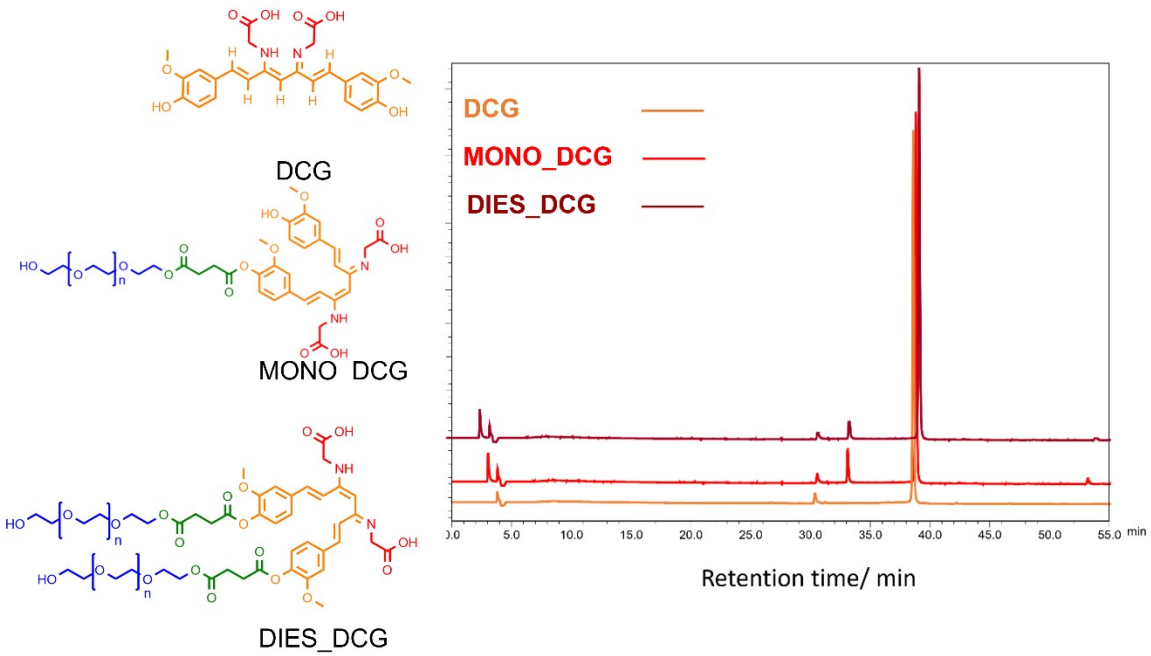

By HPLC results presented in Figure S23, MONO_DIES showed a purity of 82% (retention time at 38.6 minutes), while DIES_DCG has a purity of 80% (retention time at 38.2 minutes).

Supplementary Tables

Table S1: Reactants/ solvents used in this work.

Reactant/Solvent	Purity	Procedence
4-carboxybenzaldehyde	97%	Sigma
4-Dimethylaminopyridine	99%	Sigma
Curcumin	65%	Sigma
Curcumin	90%	-
Dichloromethane	PA	Synth
Ethanol	PA	Synth
Fumaric acid	99%	Sigma
Glycine	99%	Sigma
Maleic anhydride	99%	Sigma
N,N'-dicyclohexylcarbodiimide	99%	Sigma
PEG average M_n 8000	99%	Sigma
Succinic anhydride	99%	Sigma
Tetrachlorophthalic Anhydride	96%	Sigma
Toluene	PA	Synth
Trioctylamine	98%	Sigma
Uracil	99%	Sigma

Table S2: ^{13}C NMR signals of DCURAC.

Chemical shift	Attribution
184.9	3/3'
184.5	4a
166.8	6b
157.2	6/6'
150.2	9/9'
148.8	2a
141.4	8/8' (CUR)
141.1	5/5'
136.4	2
131.1	4b
130.9	3b
130.3	11/11'
128.2	2b
123.9	4/4'
122.3	8/8' (BDMC)
122.1	8/8' (DMC)
116.8	10/10'
116.3	7/7'
111.6	3a
101.6	1
56.3	8c/8c'

Table S3: ^{13}C NMR signals of DCURGLI.

Chemical Shift	attribution
183.3	2/2’
171.3	5a/5a'
147.9	8/8’
146.8	7/7’ (CUR)
140.6	4/4’
131.7	7/7’ (BDMC)
130.1	7/7’ (BDMC)
127.7	5/5’
122.9	10/10’
121.8	3/3’
115.9	9/9’
114.9	7/7’(DMC)
109.6	6/6’
101.3	1
55.9	7b/7b’
45.3	4a’
29.8	4a

Table S4: ^{13}C NMR signals of DCG.

Chemical shift	Attribution
183.3	2/2’
170.2	5a/5a'
147.9	8/8’
146.8	7/7’ (CUR)
140.5	4/4’
127.7	5/5’
122.9	10/10’
121.8	3/3’
115.9	9/9’
109.6	6/6’
101.3	1
65.8	4a’
55.9	7b/7b’
45.3	4a

REFERENCES

1. R.M. Silvertstain, F.X. Webter, D.J. Kiemle, D.L. Bryce, Spectroscopic Identification of Organic Compounds, eighth ed., Wiley, New York, 2015 pp-20-80.
2. C. Gaglieri, A. de Moura, R.T. Alarcon, R. Magri, G. Bannach, J. Therm. Anal. Calorim. 2022, 147, 9095-9106. https://doi.org/10.1007/s10973-022-11213-x
3. J. P. T. Baú, P. R. Anizelli, H. de Santana, M. F. da Costa, D. A. M. Zaia, Vib. Spectrosc. 2019, 101, 92–99. https://doi.org/10.1016/j.vibspec.2019.02.002
4. G. N. Ten, T. G. Burova, V. I. Baranov, J. Struct. Chem. 2007, 48, 447–455. https://doi.org/10.1007/s10947-007-0067-z
5. A. Moura, C. Gaglieri, R. T. Alarcon, L. T. Ferreira, R. Vecchi, M. L. R. Sanches, R. C. Oliveira, J. Venturini, L. C. Silva-Filho, F. J. Caires ChemistrySelect 2021, 6, 11352–11361. https://doi.org/10.1002/slct.202103359
6. A. de Moura, C. Gaglieri, L. C. da Silva-Filho, F. J. Caires, J. Therm. Anal. 2021, 146, 587–594. https://doi.org/10.1007/s10973-020-10000-w
7. A. Moura, C. Gaglieri, R. T. Alarcon, L. T. Ferreira, R. Vecchi, M. L. R. Sanches, R. C. Oliveira, J. Venturini, L. C. Silva-Filho, F. J. Caires ChemistrySelect 2021, 6, 11352 –11361. https://doi.org/10.1002/slct.202103359
8. A. de Moura, C. Gaglieri, L. C. da Silva-Filho, F. J. Caires, J. Therm. Anal. 2021, 146, 587–594. https://doi.org/10.1007/s10973-020-10000-w
9. D.W. Grijpma, Q. Hou, J. Feijen, Biomaterials. 2005, 26, 2795-2802. https://doi.org/10.1016/j.biomaterials.2004.08.002
10. R. Javahershenas, Arkivoc, 2021, 1 236–272. https://doi.org/10.24820/ark.5550190.p011.440
11. R. Madhavachary, T. Zarganes-Tzitzikas, P. Patil, K. Kurpiewska, J. Kalinowska- Tłuścik, A. Dömling, ACS Comb. Sci. 2018, 20, 192-196. https://doi.org/10.1021/acscombsci.7b00145
12. J. K. Kumar, S. Gunasekaran, S. Loganathan, G. Anand, S. Kumaresan, SAA 2013, 115, 730-737. https://doi.org/10.1016/j.saa.2013.06.097
13. S. Z. A. Ahamed, G. R. Dillip, P. Raghavaiah, K. Mallikarjuna, B. D. P. Raju, Arab. J. Chem. 2013, 6, 429-433. https://doi.org/10.1016/j.arabjc.2011.06.006
14. T. N. Drebushchak, E. V. Boldyreva, E. S. Shutova, □-Glycine. Acta Crystallogr. E: Crystallogr. Commun. 2022, E58, o634-o636. https://doi.org/10.1107/S160053680200836X